# A Novel Design for Aerial Robots to Enhance Flight Performance

Bahador Beigomi and Afshin Banazadeh

***Abstract*—In this study, a novel idea for a vertical takeoff and landing aerial robot is proposed to overcome the defects in conventional designs. Here, the coupling between translational and rotational movements that usually end up reducing flight performance and increasing control effort is eliminated by decreasing the number of main rotors and adding extra small ducted fans in an innovative scheme. The robot, named TubeDuct, can reach any position in space in a favorable horizontal attitude in order to accomplish the predefined mission with less power consumption and better performance. A linear control strategy is also proposed for this vehicle. The results are supported by nonlinear mathematical modeling and simulation, using ANSYS and MATLAB Simulink.**

***Index Terms*—TubeDuct, aerial robot, dynamic modeling, nonlinear simulation.**

## I. Introduction

Today, with the increasing scope of the activity of drones, the tendency to design and build these systems has grown dramatically, and aerial robots have a prominent role in today's societies. At present, the use and variety of perpendicular devices have increased, so that we are seeing a variety of products on different scales. These drones at small-scales have many civilian applications such as agricultural imaging, search and rescue operations, air pollution measurement and hazard detection operations for humans and numerous military applications such as subtle care, target identification, target attack, surveillance, and imaging. Increasing the usage scope of drones has increased competition in the industry. Therefore, it is necessary to create a new design that is both optimized in operational and design costs.

Behind all the military and civilian missions defined for aerial robots, there is a need to improve existing drones in terms of improved functional capabilities as well as reduced energy consumption. One way forward is to change how the rotors are arranged. There are many different designs in the area of multi-rotors, the most important and famous of which is Quadrotor. Although quadrotor has several advantages, including ease of construction and ease of control, it has weaknesses in terms of energy consumption as well as coupling between positional and transient modes. Therefore, the main purpose of this research is to design and develop a novel aerial vehicle that, in addition to having the common advantages of being able to take-off and land vertically, or stable flight, would be more favorable in other contexts, such as being able to fly in the horizon plane without changing the attitude parameters.

So far, there has not been a direct and explicit design similar to this project design. In the past decades, various control ideas and techniques have been developed to better capture aerial robots, relying on enhanced functionality in flight. Advances in microelectromechanical systems and sensors have led to better control methods and mechanisms. Examples include planning and controlling overcast air maneuvers [1], controlling small robots and flying micro-robots [2], and predicting spontaneous flight modes [3].

Also, in recent years, researchers have tried to adjust the number of control parameters of the system to its degrees of freedom. These adjustments change the robots to fully actuated or even over-actuated. One of the suggested methods is to change the angle of the engine/blades of an aerial robot, which however generates gyroscopic moments and thus tightens drone controllability [4], [5]. Changing the number of blades and their shape has led to a variety of ideas for building and controlling aerial robots with three blades [6], [7].

Also, by attempting to modify the overall shape of the multi-rotor aerial robots, an attempt was made to resolve the under-actuated problem [8]. Of course, increasing the number of motors can also be a solution to the out-of-action situation [9]. The basic idea of the designed aerial robot to be explored in this study is taken from the Omnicopter [10], [11].

In this study a complete model is developed, using Ansys to determine the forces and moments applied to the TubeDuct and a simulation environment is developed to evaluate the equations of motion and analyze the presented model in MATLAB Simulink.

## II. TubeDuct Description and Conceptual Design

Nowadays, different missions can be implemented for aerial robots and depending on the mission, different models can be designed and built. For example, the aerial robot used to extinguish a fire differs markedly in design from the aerial robot used for regional monitoring.

Since the main purpose of this project is to design a flying vehicle that can easily be commuted to different locations, the design of its components must also be such that it is suitable for delivering the goods with minimum damage to its payload. Table 1 is adequately and precisely comparing all available types of multi-rotors to find the best type for our mission purpose, which is delivery.

As shown in Table I, the use of coaxial multi-rotors is more desirable because of the following performance

Manuscript received February 26, 2020; revised April 1, 2020.

Bahador Beigomi is with Sharif University of Technology, Tehran, Iran (e-mail: bahador.beigomi@gmail.com).

Afshin Banazade is with Aerospace Eng. Dept., Sharif University of Technology, Tehran, Iran (e-mail: banazadeh@sharif.edu).

DOI: 10.7763/IJMO.2020.V10.752

characteristics:

The use of coaxial rotors increases the efficiency of the blades and also increases the power output [13].

The most important performance characteristic for a delivery drone is its ability to move horizontally in the horizontal plane without changing its level position. This will increase the efficiency of the drone's movement. Clearly, the battery, motor, and propeller assemblies each have the highest efficiency at a given speed, and by removing each of these components from the rated range, the efficiency of the drone decreases.

Table 1. Comparison of Multi-Rotors (VTOL) (1=Bad, 4=Very Good)[12]

TABLE I: COMPARISON OF VTOL MULTI-ROTORS (1=BAD, 4=VERY GOOD) [12]

| | Axial Rotor | Coaxial | Quad Rotor | Hexa Copter | Tri Copter | Heli Copter |
|---|---|---|---|---|---|---|
| Power Cost | 4 | 4 | 3 | 2 | 4 | 2 |
| Control Cost | 2 | 4 | 4 | 3 | 2 | 2 |
| Payload capability | 3 | 4 | 3 | 4 | 2 | 4 |
| Maneuverability | 1 | 3 | 4 | 4 | 2 | 2 |
| Mechanical Simplicity | 3 | 4 | 4 | 2 | 3 | 1 |
| Aerodynamics Complexity | 1 | 1 | 4 | 2 | 3 | 1 |
| In-plane Maneuverability | 2 | 4 | 1 | 1 | 1 | 1 |
| Low speed flight | 4 | 4 | 4 | 4 | 4 | 4 |
| High speed flight | 1 | 1 | 3 | 4 | 2 | 2 |
| Flying in all Weather | 3 | 3 | 2 | 2 | 2 | 2 |
| Miniaturization | 3 | 4 | 4 | 2 | 3 | 2 |
| Survivability | 1 | 3 | 2 | 4 | 2 | 1 |
| Stationary flight | 3 | 4 | 4 | 4 | 4 | 4 |
| People Safty | 3 | 4 | 2 | 2 | 3 | 1 |
| Total | 34 | 47 | 44 | 40 | 37 | 29 |

Due to the interaction of delivery aerial robots with customers, these flying vehicles must be highly secure during takeoff and landing. Multi-rotors, such as the Quadrotor, whose blades are usually out of body, face a safety problem for close ones. Also, in dense urban areas it is possible to hit foreign objects such as the foliage of trees, which will cause the drone to fall.

In Fig. 1(a), the position of the main rotors, ducts of the side fans, control surfaces and other flying components is well represented. The TubeDuct has the vertical take-off and landing ability while it can move in-plane smoothly without changing its desired position.

In Fig. 1(b), aerial robot components are visible. Two central coaxial motors are for generating aerial robot vertical force, two ducted-fans located on both sides of the robot have the task of generating the power to move on the plane, and two block surfaces located under coaxial rotors have the sole purpose of stabilizing the aerial robot and two boxes designed for carrying TubeDuct's payload.

## III. MATH

The overall appearance of the TubeDuct resembles a donut and has attempted to produce as little drag force as possible. This minimum drag force is due to the outer shape of the TubeDuct. The outer wall of the TubeDuct is a slice of the NACA0025 Airfoil, starting at the nose of the airfoil and continuing to the thickest of the airfoil. Therefore, at different horizontal velocities, there is no separation of the stream until the flow reaches the center crater. Also, in full horizontal mode, the body does not generate lift force, which results in no asymmetric lift force on the TubeDuct.

The central component consists of two motors, two coaxial blades with opposite rotation, and four control blocks. Coaxial blades have a distance of about 2.5cm from each edge of the central duct, which is sufficient distance to provide adequate thrust force [14].

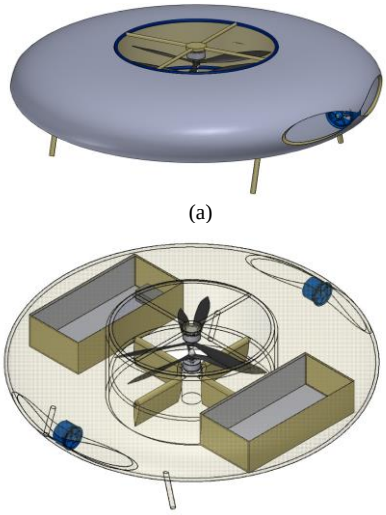

(a)

(b)

Fig. 1. Tube duct schematic.

NACA0018 symmetric airfoils are also used in the control surfaces to produce the lowest drag force at zero angle of attack. Fig. 2 shows the central components of the TubeDuct, consisting of two main motors, two coaxial blades, and control surfaces.

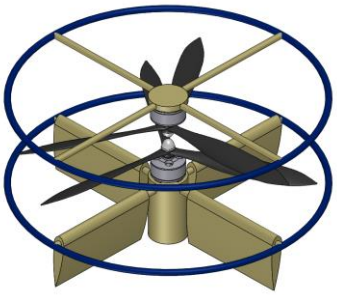

Fig. 2. Central components of the TubeDuct.

TABLE II: MAIN DESIGN CHARACTERISTICS OF THE TUBEDUCT

| variable | value |
|---|---|
| Outer frame airfoil | NACA0025 |
| Control Surfaces airfoil | NACA0018 |
| Mass [kg] | 3.5 |
| $I_{xx}\lfloor kg.m^2 \rfloor$ | 0.22 |
| $I_{yy}\lfloor kg.m^2 \rfloor$ | 0.23 |
| $I_{zz}\lfloor kg.m^2 \rfloor$ | 0.42 |
| $I_{xy}\lfloor kg.m^2 \rfloor$ | -0.06 |
| Control Surface Area[$m^2$] | 0.2 |
| Number of Blades | 3 |
| Ducted-fan Diameter[m] | 0.07 |
| Outer diameter [m] | 1 |
| Inner diameter [m] | 0.5 |

The control surfaces are located at the lowest part of the TubeDuct's enclosed middle space to be as far as possible to the center of gravity of the TubeDuct. So, as a result, produce the highest momentum with the lowest angle deflection. The way these control surfaces move is that the two surfaces rotate in the same direction at the same speed and value. Only

one servo is provided to control the angle of each pair of opposing surfaces. Table II lists the geometrical and physical parameters of the TubeDuct.

## IV. Dynamic Modeling

In this section, the nonlinear dynamics modeling of the TubeDuct in six degrees of freedom will be discussed, followed by a system to control the orientation and position of the TubeDuct. The coordinate systems and free body diagram for the TubeDuct are shown in Figure 3. The inertial frame $I = \lfloor I_x \quad I_y \quad I_z \rfloor$ is considered fixed with respect to the earth, with axis $I_z$ pointing downward. Let $B = \lfloor B_x \quad B_y \quad B_z \rfloor$, which is attached to the center of mass of the TubeDuct aerial robot, the body frame, where the $B_x$ axis is in the forward flight direction, $B_y$ is perpendicular to $B_x$ and positive to the right in the body plane, whereas $B_z$ is orthogonal to the plane formed by $B_x$ and $B_y$. $B_z$ points vertically downwards during perfect hover. We use Z-Y-X Euler angles to model the rotation of the TubeDuct aerial robot in the inertial frame. The airframe orientation is given by a rotation matrix $R^{BI}$, where $R \in SO(3)$ is an orthonormal rotation matrix. To get from $B$ to $I$, we first rotate about $B_z$ by the yaw angle $\psi$, then rotate about the intermediate Y-axis by the pitch angle $\theta$, and finally rotate about the $I_x$ axis by the roll angle $\phi$. This rotation matrix is given by [15]:

$$R^{BI} = \begin{bmatrix} c\theta c\phi & c\psi s\theta s\phi - s\psi c\phi & c\psi s\theta c\phi + s\psi s\phi \\ c\theta s\phi & s\psi s\theta s\phi + c\psi c\phi & s\psi s\theta c\phi - c\psi s\phi \\ -s\theta & s\psi c\theta & c\psi c\theta \end{bmatrix} \quad (1)$$

The derivatives with respect to time of the roll, pitch and yaw angles can be expressed in the form

$$\begin{bmatrix} \dot{\phi} \\ \dot{\theta} \\ \dot{\psi} \end{bmatrix} = \begin{bmatrix} 1 & \sin\phi\tan\theta & \cos\phi\sin\theta \\ 0 & \cos\phi & -\sin\phi \\ 0 & \sin\phi\sec\theta & \cos\phi\sec\theta \end{bmatrix} \begin{bmatrix} p \\ q \\ r \end{bmatrix} \quad (2)$$

where, $\lfloor p \quad q \quad r \rfloor^T$ is the angular velocity in the body frame.

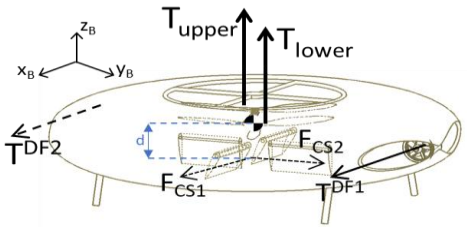


Fig. 3. TubeDuct free body diagram.

The basic assumptions used in developing TubeDuct dynamic model include: mass and moments are assumed to be constant, upper and lower saturation on each control, incompressible air flow, and the effects of side fans are not considered in the aerodynamic forces due to their small size.

$$F^B = \begin{bmatrix} T^{DF} + L^{CS1} - D_x^{Body} \\ L^{CS2} - D_y^{Body} \\ T^{upper} + T^{lower} - D_z^{Body} - D^{CS1} - D^{CS2} \end{bmatrix} \quad (3)$$

In the above equation, $T^{upper}$ and $T^{lower}$ are thrust forces generated by the central rotors, $D^{Body}$ is body drag force, $D^{CS}$ and $L^{CS}$, are drag force and lift force, respectively, produced by the control surfaces. $T^{DF}$ is also the force produced by the side ducts, which are always aligned along the x body axis.

How to obtain the elements of Eq. (3) is that first, the aerodynamic forces, such as the flying force or forces generated by the control surfaces, are simulated by Fluent software at different speeds with acceptable accuracy. An example of this test is illustrated in Fig. 4. Second, the calculation of the force generated by the central rotors ($T^{upper}$ and $T^{lower}$) is performed using the blade element momentum theory [16]. In fact, the blade element momentum theory at any moment of flight using the rotational speed of motors and physical parameters of the blades such as the diameter, step, number of blades, etc., to calculate the thrust force and torque generated and produced by each rotor.

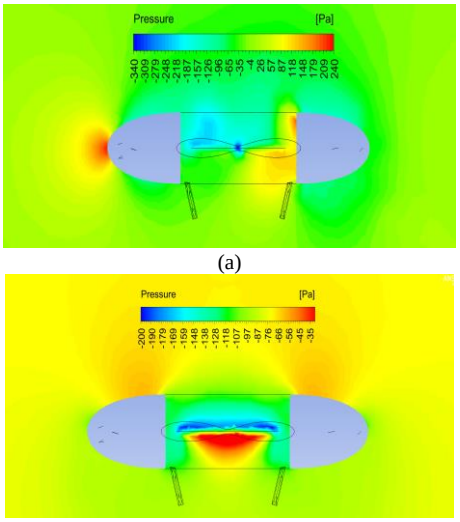


(a)

(b)

Fig. 4. Calculating drag force with Fluent in (a) level flight (b) vertical flight

External moments on the TubeDuct in the body coordinate are as follows:

$$M^B = \begin{bmatrix} M_x^{gyro} + M^{CS2} \\ M_y^{gyro} + M^{CS1} \\ M^{prop} \end{bmatrix} \quad (4)$$

In the following, we will examine each of the elements of Eq. (4). The gyroscopic momentum results from the rotational speed difference of the central rotors. If there is a rotational velocity difference and the TubeDuct is rotating around the x or y axis, then gyroscopic momentum is created.

$$M^{gyro} = \begin{bmatrix} I_p \omega_y \left(\Omega_{upper} - \Omega_{lower}\right) \\ I_p \omega_x \left(\Omega_{lower} - \Omega_{upper}\right) \\ 0 \end{bmatrix} \quad (5)$$

In Eq(5), $\Omega_{upper}$ and $\Omega_{lower}$ are rotational speed of the up and down rotors respectively, $\omega_x$ and $\omega_y$ are the rotational speed of the TubeDuct around the x and y axes, and finally $I_p$ is the moment of inertia of the central blades for which this value is 1.5e-3. Although the momentum due to the gyroscopic effect is negligible, it is intended to increase modeling accuracy.

The next term to be examined is the momentum on the body by the control surfaces. As noted earlier, control surfaces produce a force in the x and y body coordinate system. The forces generated by the control surfaces do not enter the center of mass and there is a distance (d) between the place that forces effect and center of mass. This non-alignment causes the momentum generated by the control surfaces to return the TubeDuct to equilibrium.

$$M^{CS} = \begin{bmatrix} L^{CS2} d \\ L^{CS1} d \\ 0 \end{bmatrix} \tag{6}$$

In Eq(6), $L^{CS}$ is the lift force applied by the control surfaces. Also, d is the arm of these forces, which is the distance from the center of pressure of these surfaces to the center of mass of the TubeDuct and is about 1.5 cm.

The last term in Eq(4) is the moment in the z-direction of the body coordinate. $M^{prop}$, results from the difference in rotational speeds of the main TubeDuct blades. The momentum generated by the central rotors, like their thrust force, is obtained by the blade element momentum theory.

Finally, the equations of motion are obtained as follows.

$$\begin{cases} \dot{x} = v \\ \dot{v} = mge_3 + F^B \\ \dot{R}_{Rot} = R_{Rot}.sk(\omega) \\ J\dot{\omega} = -\omega \times J\omega + M^B \end{cases} \tag{7}$$

where, $v$ is velocity in the inertial frame, $e_3 = \begin{bmatrix} 0 & 0 & 1 \end{bmatrix}^T$, and

$$sk(\omega) = \begin{bmatrix} 0 & -\omega_z & \omega_y \\ \omega_z & 0 & -\omega_x \\ -\omega_y & \omega_x & 0 \end{bmatrix}, \quad J = \begin{bmatrix} I_{xx} & I_{xy} & 0 \\ -I_{xy} & I_{yy} & 0 \\ 0 & 0 & I_{zz} \end{bmatrix} \tag{8}$$

## V. Control Design

How to control the TubeDuct is that the flight altitude is first adjusted and then the angle of the TubeDuct (its point of view) is adjusted in the proper direction and after zeroing the side angle error, it moves to the appropriate location using the side ducts-fan. This is, in fact, the whole way of how to move from point to point.

This section first describes how to set control gains for the controllers listed in the linearized dynamic model of the TubeDuct. Then the obtained coefficients applied to the nonlinear system and, by trial and error, the system response will be optimized. After obtaining the desired coefficients, various missions are executed on the system and the results are obtained from the simulation model.

• Control Surfaces

As mentioned, control surfaces have the task of preventing TubeDuct rotation around the x and y axes. The system first linearizes around the defined working point to prevent the TubeDuct from rotating around the y-axis. This is done by the control surface1. For linearization it is assumed that $I_{xy} = 0$. The linearized system for control surface1 is as follows.

$$x = \begin{bmatrix} q & \theta \end{bmatrix}, \dot{x} = Ax + Bu \rightarrow A = \begin{bmatrix} 0 & 0 \\ 1 & 0 \end{bmatrix}, B = \begin{bmatrix} 0.1428 \\ 0 \end{bmatrix} \tag{9}$$

In order that the system response to be optimized, the overshoot and the system settling time are considered 1% and 2 seconds, respectively. Using these two parameters, the desired poles of the system are obtained.

$$\xi = \sqrt{\frac{(\ln os)^2}{\pi^2 + (\ln os)^2}} \xrightarrow{os=2\%} \xi = 0.78 \tag{10}$$

$$T_s = \frac{3.9}{\xi \omega_n} \xrightarrow{T_s=1} \omega_n = 5 \tag{11}$$

Using the parameters obtained in Eqs (9), (10) and (11), and by the Ackermann's formula, the control gains of the control surface #1 will be[17]:

$$u = -Kx \rightarrow u = -\begin{bmatrix} 56.62 & 175.07 \end{bmatrix} \begin{bmatrix} q \\ \theta \end{bmatrix} \tag{12}$$

Using the same way to calculate control gains for the Control surface #2, the result is as follows:

$$u = -Kx \rightarrow u = -\begin{bmatrix} 52.03 & 166.77 \end{bmatrix} \begin{bmatrix} p \\ \phi \end{bmatrix} \tag{13}$$

• Altitude and yaw angle

From TubeDuct dynamics can be concluded that two main rotors are used to control the flight altitude as well as the yaw angle. The inputs to this control system are angular velocities of the TubeDuct's central blades. We use the Ziegler-Nichols method to obtain appropriate initial guesses for the control coefficients of the system [18]. To control the flight altitude and yaw angle of the TubeDuct, there is no need for the integrator term and only with the PD controller we can get the desired results. The appropriate control gains obtained from the Ziegler-Nichols method are as follows.

TABLE III: Appropriate Control Gains Obtained by the Ziegler-Nichols Method

| | $K_p$ | $K_d$ |
|---|---|---|
| Altitude control | 320 | 110 |
| Yaw angle control | 2900 | 1500 |

TABLE IV: Control Gains to Reach Optimal Flight Performance

| | $K_p$ | $K_d$ |
|---|---|---|
| Altitude control | 368 | 138 |
| Yaw angle control | 3400 | 2700 |

The control gains obtained by the Ziegler-Nichols method are in fact an initial conjecture of the control gains. To obtain proper control gains, we use trial and error to perform system behavior appropriate to the desired flight performance. Designed for optimal flight performance, reducing system overshoot as well as reducing system response time. The optimal gains are shown in Table IV.

The reason for the high yaw angle control gains is that a slight change in the angle of rotation of the main rotors cannot cause the TubeDuct to rotate rapidly around the body axis.

- Horizontal position

TubeDuct horizontal position control, begins after the zero error of altitude and yaw angle. The two small ducts mounted on the TubeDuct have the task of moving to the target point. As the side angle error becomes zero, the two ducted-fans light up and move the TubeDuct in x direction. The linear motion, due to the zero-angle error will be completed towards the target point. In order to be able to fix the TubeDuct at the endpoint, it is necessary to stop the ducted-fans before reaching the endpoint. After this, the drag force will slow down the TubeDuct at the desired final point.

## VI. Simulation Results

In the nominal mission scenario, the TubeDuct must cross along the route, and chooses a straight path between two points. If the two points are not at the same height, TubeDuct's height is initially adjusted and then it rotates to reach the target direction. If TubeDuct faces turbulence, the controller has a function of zeroing roll and pitch angles through an inner closed-loop system, no matter what type and how the mission is performed. The zeroing of these angles, carried out by the control surfaces, is accompanied by a slight change in the TubeDuct's location. This shift will cause TubeDuct's yaw angle to change momentarily. The altitude control and yaw angle control system, controlled by the same inputs, simultaneously adjusts the TubeDuct's altitude to the desired altitude and direction to the target point at any moment. To verify the designed controllers, the results of a delivery mission are presented in this paper. Here, there must be at least two target points for the TubeDuct. To check the proper operation of the control surfaces, we divert the TubeDuct around the x body axis by 15 degrees. All along the way, we also assume that a torque of 1.5 N.m. is acted to the TubeDuct around the y body axis. Assume that the initial position is $\begin{bmatrix} x_0 & y_0 & z_0 \end{bmatrix}_{(m)}^T = \begin{bmatrix} -800 & 2350 & 0 \end{bmatrix}^T$ and initial attitude is $\begin{bmatrix} \phi_0 & \theta_0 & \psi_0 \end{bmatrix}_{(\deg)}^{\circ} = \begin{bmatrix} 15^{\circ} & 0^{\circ} & -143^{\circ} \end{bmatrix}^T$ and all the linear and angular velocities are zero. Four desired point for this mission will be:

$$\begin{bmatrix} x_{des} & y_{des} & z_{des} \end{bmatrix}_{(m)}^T$$
$$\rightarrow \begin{bmatrix} 140 & 1050 & 150 \end{bmatrix}_1^T \rightarrow \begin{bmatrix} 310 & 1050 & 150 \end{bmatrix}_2^T$$
$$\rightarrow \begin{bmatrix} 600 & 400 & 150 \end{bmatrix}_3^T \rightarrow \begin{bmatrix} 600 & 400 & 0 \end{bmatrix}_4^T$$

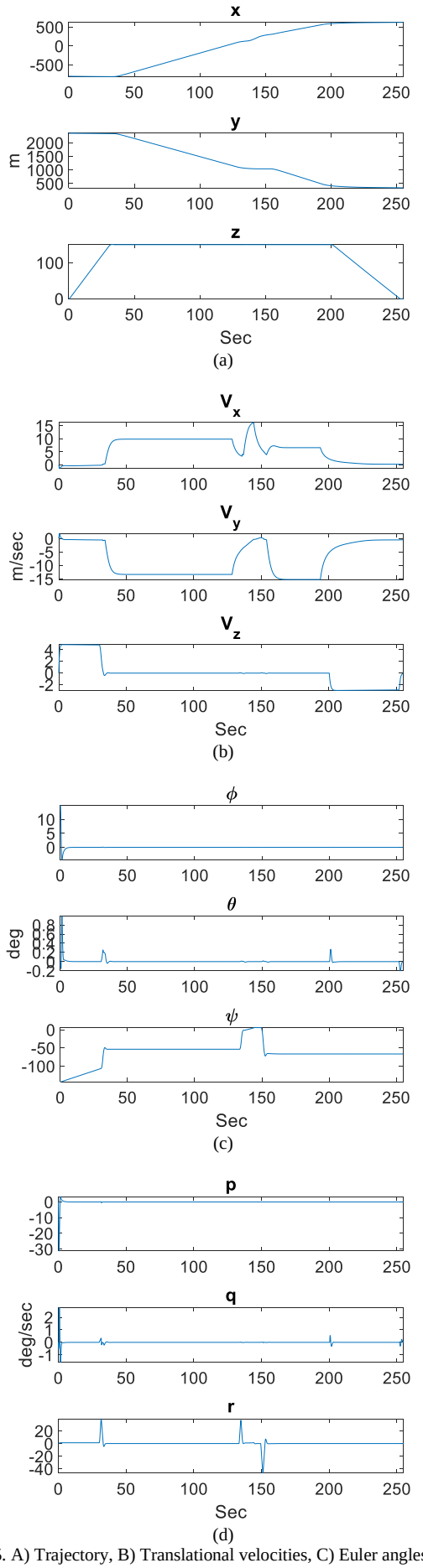


Fig. 5. A) Trajectory, B) Translational velocities, C) Euler angles, and D) Angular velocities.

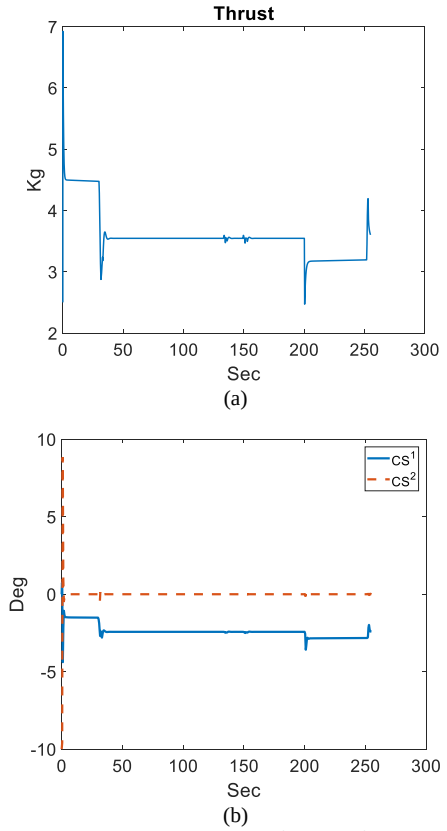


Fig. 6. A) Coaxial rotor thrust, B) Deflection of control surfaces.

## VII. Concluding Remarks

In this paper, design of a novel aerial robot, TubeDuct is proposed. It is unique in its ability to fly in any direction without changes in its attitude. The conceptual design of the TubeDuct sought to take into account several advantages, such as low drag, vertical take-off and landing capability, the possibility of horizontal movement with no change in attitude, and a safe cargo compartment. A nonlinear dynamic model of this aerial robot is established and a linear controller has been designed for a nominal mission. The optimal control gains are also calculated from linearized dynamic model. The simulation results prove that the position and attitude stabilization task of the TubeDuct is achieved in the presence of external disturbances. A prototype will be constructed in the future, and various control strategies will be experimentally validated on the platform.

## Conflict of Interest

The authors declare no conflict of interest.

## Author Contributions

Both authors contributed substantially to the conception and design of the study and approved the final version. A.B. suggested the main idea and supervised the research. B.B. conducted the research, analyzed the data, and co-wrote the paper.

## References

[1] D. Mellinger, N. Michael, and V. Kumar, "Trajectory generation and control for precise aggressive maneuvers with quadrotors," *The International Journal of Robotics Research*, 2012, vol. 31, no. 5, pp. 664-674.

[2] J. Winslow *et al*., "Design, development, and flight testing of a high endurance micro quadrotor helicopter," *International Journal of Micro Air Vehicles*, 2016, vol. 8, no. 3, pp. 155-169.

[3] S. Shen *et al.*, *Vision-Based State Estimation and Trajectory Control Towards High-Speed Flight with a Quadrotor*, in *Robotics: Science and Systems*, 2013.

[4] M. Ryll, H. H. Bülthoff, and P. R. Giordano, "A novel overactuated quadrotor unmanned aerial vehicle: Modeling, control, and experimental validation," *IEEE Transactions on Control Systems Technology*, 2015, vol. 23, no. 2, pp. 540-556.

[5] K. T. Öner *et al*., "Dynamic model and control of a new quadrotor unmanned aerial vehicle with tilt-wing mechanism," 2008.

[6] S. K. Sai and H. M. Tun, "Modeling and analysis of tri-copter (VTOL) aircraft," *International Journal*, 2015, vol. 54.

[7] D. W. Yoo *et al*., "Dynamic modeling and control system design for tri-rotor UAV," in *Proc. 2010 3rd International Symposium on Systems and Control in Aeronautics and Astronautics*, 2010.

[8] Y. Long and D. J. Cappelleri, "Complete dynamic modeling, control and optimization for an over-actuated MAV," in *Proc. 2013 IEEE/RSJ International Conference on Intelligent Robots and Systems*, 2013.

[9] X. J. Chen *et al*., "Optimal type II Fuzzy neural network controller for eight-rotor MAV," *International Journal of Control, Automation and Systems*, 2017, vol. 15, no. 4, pp. 1960-1968.

[10] Y. Long and D. J. Cappelleri. "Linear control design, allocation, and implementation for the omnicopter mav," in *Proc. 2013 IEEE International Conference on Robotics and Automation (ICRA)*, 2013.

[11] Y. Long and D. J. Cappelleri, "Omnicopter: A novel overactuated micro aerial vehicle," *Advances in Mechanisms, Robotics and Design Education and Research*. 2013, Springer. pp. 215-226.

[12] S. Bouabdallah, M. Becker, and R. Siegwart, "Autonomous miniature flying robots: coming soon!-research, development, and results," *IEEE Robotics & Automation Magazine*, 2007, vol. 14, no. 3, pp. 88-98.

[13] Y. Jiang, H. Li, and H. Jia, "Aerodynamics optimization of a ducted coaxial rotor in forward flight using orthogonal test design," *Shock and Vibration*, 2018.

[14] D. E. Brody *et al*., *Coaxial Rotor Aircraft*, 2012, Google Patents.

[15] J. Roskam, *Airplane Flight Dynamics and Automatic Flight Controls*, 1998.

[16] F. Bohorquez *et al*., "Design, analysis and hover performance of a rotary wing micro air vehicle," *Journal of the American Helicopter Society*, 2003, vol. 48, no. 2, pp. 80-90.

[17] K. Ogata and Y. Yang, *Modern control Engineering*, vol. 5. 2010.

[18] J. Zhong, "PID controller tuning: A short tutorial," *Mechanical Engineering*, Purdue University, 2006, pp. 1-10.



**Bahador Beigomi** obtained his BSc and the MSc in aerospace engineering at Sharif University of Technology, Tehran, Iran. He worked there as a research assistant for two years. He is currently PhD candidate at York University, Toronto, Canada. His research interests are around aerial robotics and robot kinematics.

**Afshin Banazadeh** joined the Department of Aerospace Engineering at Sharif University of Technology (SUT); Tehran, Iran in 2009. He received his Ph.D. in aerospace engineering; flight dynamics and control, from SUT in 2008. Banazadeh has performed his sabbatical research at Cranfield University, Bedfordshire, England; primarily focusing on the characterization of co-flow fluidic thrust vectoring for use on air vehicles. He is the founder and director of Shenasa Systematic Design Group at Sharif Tech-ology Service Complex and expanded the group in the area of system design, simulation and testing. His research and teaching interests have focused on aircraft design, system identification, flight dynamics, flight test engineering, and technology demonstration activities. He has published over 60 scientific articles in peer-reviewed reputable journals and conferences and served as a reviewer for many professional journals including aerospace science and technology, IEEE transactions on automatic control, ocean engineering, and plos one. He has also served on scientific committee of several national/international conferences. His current interests are fault tolerant control, visual servoing, and adaptive neuro-controllers. His research mission is to address existing and emerging challenges facing autonomous air vehicles operating in civil airspace.